

## Model for Intrinsic Stress Formation in Amorphous Thin Films

S. G. Mayr\* and K. Samwer

*I. Physikalisches Institut, Bunsenstrasse 9, D-37073 Göttingen, Germany*

(Received 8 December 2000; published 2 July 2001)

Metallic amorphous thin films evaporated on a substrate can be characterized by different growth regimes in dependence of the film thickness concerning surface morphology and intrinsic film stresses, independent of the details of the applied material systems. Here, a model is presented to link the surface topography and characteristic surface measures with the observed film stresses. This allows quantitative prediction of stresses in dependence of film preparation parameters for a tailored film production.

DOI: 10.1103/PhysRevLett.87.036105

PACS numbers: 68.55.-a, 61.43.Dq, 68.35.Gy

Despite their structural similarity to liquid melts on an atomic scale, amorphous thin films evaporated on substrates held far below the glass transition temperature do not reveal liquidlike features on a mesoscopic or macroscopic scale, mainly due to a finite shear modulus. This is experimentally evident from the pronounced structure formation observable in scanning tunneling microscopy (STM) growth studies [1–3], especially in the high film thickness regimes of several 100 nm film thickness, and the permanent buildup of intrinsic growth stresses of both signs in the different stages of film growth [4]. In contrast to crystal systems, amorphous thin films possess no long range structural order without any crystal anisotropy and do not allow typical crystal relaxation mechanisms, such as dislocation creep, which makes them the ideal model-system for film growth concerning surface morphology and film stresses, independent of the details of the substrate for sufficient film thicknesses. Particularly, a direct relation of morphology and stresses and a modeling of surface morphology and stress evolution during film growth can thus be expected to be possible.

Experimentally, amorphous thin films are coevaporated by independently rate-controlled electron-beam evaporators under ultrahigh vacuum (UHV) conditions ( $2 \times 10^{-10}$  mbar) onto single-edge fixed oxidized Si(100) substrates, and a two laser-beam deflection method is used for *in situ* stress measurements. UHV-STM investigations are performed after transfer of the sample to a different chamber without breaking the vacuum. Figure 1 shows the substrate curvature for a stress measurement during the deposition of a ternary amorphous  $Zr_{65}Al_{7.5}Cu_{27.5}$  film, using the convention of positive curvature for compressive stresses. Concerning the incremental stresses (proportional to the derivation with respect to the film thickness  $t$ ) a very thin film tensile region, a compressive regime for medium film thicknesses, and tensile stresses for high film thicknesses can be distinguished. The surface morphology  $h(x, y)$  (on a two dimensional coordinate system in the plane of a substrate) in the transition region from compressive to late-stage tensile stresses is accessible with the STM growth studies (Figs. 2c and 2d). It shows qualitatively an enhanced broadening and an increase in

height of the clusterlike surface structures. Quantitatively, this coincides with the maximum increase of the surface roughness

$$\zeta = \sqrt{\langle [h(x, y) - \langle h(x, y) \rangle]^2 \rangle} \quad (1)$$

with the film thickness and the saturation of the lateral structure sizes  $R_C$  (Fig. 1—data points from [1] are also included) determined from the abscissa of the first maximum of the height-height-correlation functions

$$C(r) = \langle h(\vec{x})h(\vec{x} + \vec{R}) \rangle_{\vec{x}; |\vec{R}|=r} \quad (2)$$

with  $\vec{x} = (x, y)$ . In contrast, the transition from the early-stage tensile to compressive stresses can be measured only on a HOPG (highly oriented pyrolytic graphite) [2] due to conductivity problems on  $SiO_2$ , showing a coalescence phenomenon of single islands (Figs. 2a and 2b). However, the conductivity problems themselves show not only island growth, but also coalescence on  $SiO_2$ , as follows from the onset of conductivity. This is additionally corroborated by

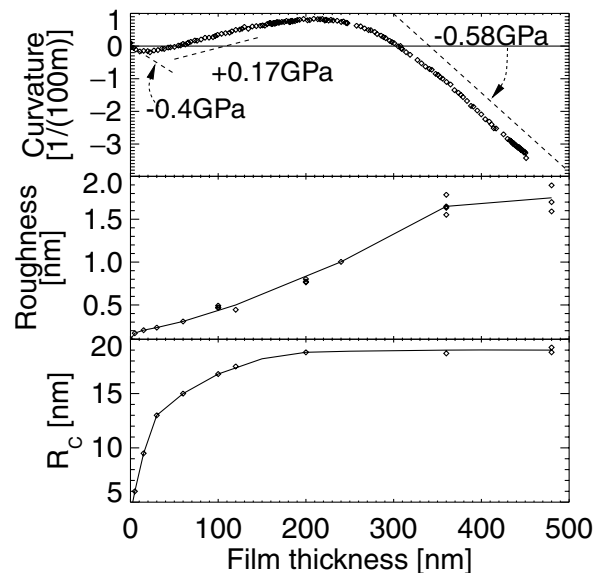


FIG. 1. Evolution of substrate curvature, roughness, and lateral structure size  $R_C$  with film thickness for amorphous  $Zr_{65}Al_{7.5}Cu_{27.5}$  films.

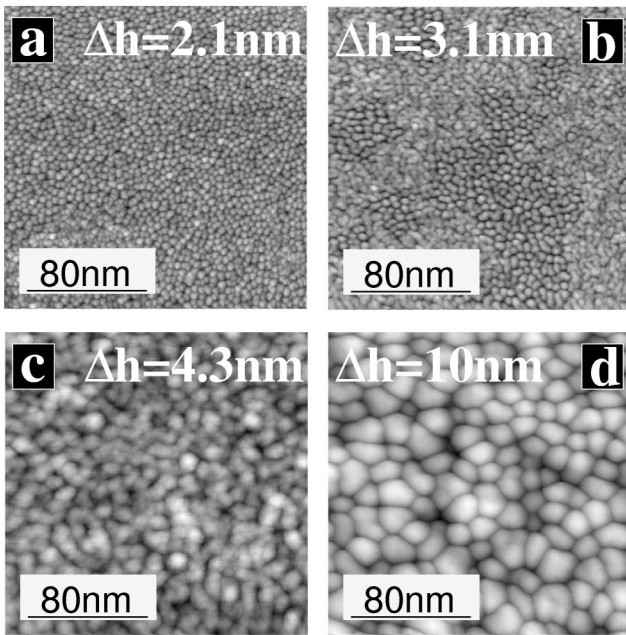


FIG. 2. Ultrathin  $Zr_{65}Al_{7.5}Cu_{27.5}$  films on HOPG show island growth and coalescence [(a) 0.8 nm; (b) 5.0 nm]. With increasing film thickness a clusterlike surface with coalescence evolves [(c) 100 nm; (d) 480 nm].

conductivity measurements during the evaporation of comparable amorphous alloys [4]. The described surface structure and stress correlations are common with other studies on binary amorphous metals, showing an independence of the measured compressive stresses of the surface morphology and temperature, and a scaling of the late-stage tensile stresses with the reciprocal lateral structure sizes, independent of the details of the early stages of film growth [5].

The independence of morphology and stresses of the details of the substrate, except for the very early stages of film growth, suggests atomic dynamics during particle deposition to be the only reason for the observed phenomena, i.e., the propagation of the film-vacuum interface through the film with different surface morphologies. As could be shown by a quantitative modeling of amorphous film growth [3,6], it is mainly based on kinetic-induced growth instabilities (self-shadowing) and energy minimization. However, energy minimization by atom diffusion, as considered in the previous models, is not the only way of minimizing local energy. The idea now is to relate other, nondiffusional energy minimizing mechanisms at the surface to the generation of film stresses. This is in contrast to stress-induced surface modification by externally applied or lattice-mismatch-induced film stresses for crystal systems, which is based on directed diffusion from the valleys to the top of the hills of the surface structures due to stress-induced changes in local chemical potentials (e.g., the Asaro-Tiller-Grinfeld instability [7]).

Morphology independent energy reduction at a surface can arise by surface reconstruction changing the surface packing density: In solids the surface stress  $f$  and the sur-

face energy  $\gamma$  have to be distinguished [8]. The difference, according to the Shuttleworth equation [9] with the biaxial strain  $\epsilon$ ,

$$\frac{\partial \gamma}{\partial \epsilon} = 2(f - \gamma), \quad (3)$$

is the driving force for a modification of the surface packing density, known to cause surface reconstruction in crystal systems [10,11]. Here, the elastic energy per area

$$W_{\text{elastic}} = Bt_0\epsilon^2 \quad (4)$$

( $t_0$ : thickness of the surface layer) and the misfit energy to the bulk counteract. In amorphous systems with numerous energetically equivalent, almost randomly distributed positions on the surface, the misfit energy in the case of surface reconstruction should be negligible. In the case of sufficient low adatom mobility, the modified adatom density can be propagated into the interior of the film, leading to biaxial film stresses

$$\sigma = (f - \gamma)/t_0. \quad (5)$$

In most metal systems,  $f - \gamma$  is positive [11], leading to compressive stresses. Taking the atomical roughness observable in a typical amorphous film as an estimate for  $t_0$ ,

$$f - \gamma \approx 0.17 \frac{N}{m} \quad (6)$$

can be estimated from the medium film thickness regime in Fig. 1.

In the case of rough cusplike surfaces, such as single islands on top of a substrate or the clusterlike surface in the high film thickness regime (Fig. 1), the energy might be reduced by processes joining the cusp walls together, generating strain, as inverse Griffith crack theory, as suggested by Nix and Clemens [12,13]. However, a pure static closure of the cracklike cusps, leading to extremely high stresses, seems idealized from the experimental or simulation point of view as local relaxation processes will be able to reduce stresses. A hint concerning the type of relaxation can be achieved by considering the radially averaged spectral power density

$$C(q, t) = \langle |h(\vec{q}, t)|^2 \rangle_{|\vec{q}|=q} \quad (7)$$

as calculated from the STM topographs for a 480 nm thick film [ $h(\vec{q}, t)$  denotes the spatial Fourier transformation of the surface topograph  $h(\vec{x}, t)$ —Fig. 3]. In the long-time limit it has the interesting property of showing a power-law behavior (with constants  $a_i$ )

$$C(q) \propto \frac{1}{\sum_{i=1}^4 a_i q^i} \quad (8)$$

with exponents characteristic for atomic processes on top of film surfaces [14,15]. It reveals—beside the diffusional  $q^{-4}$  decrease *on top of* the hills—a  $q^{-1}$  decrease for spatial frequencies  $q$  *between* two hills, characteristic for viscous flow. Extensive molecular dynamics simulations on nanocluster sintering indeed show a viscous sintering between clusters far below the melting temperature [16].

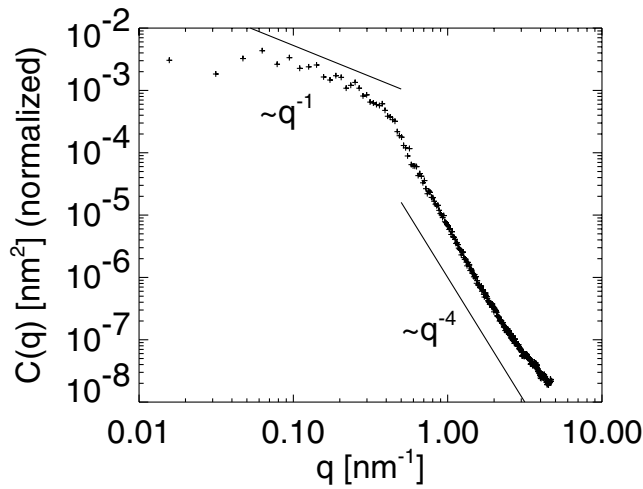


FIG. 3. Spectral power density, calculated from an STM measurement of a 480 nm thick  $Zr_{65}Al_{7.5}Cu_{27.5}$  film. The lines indicate the different power laws of  $q$ .

Assuming a continuous viscous coalescence mechanism of the clusterlike late stages of film growth to a cycloidlike surface with the hills tightly bound to the rest of the film, the stress can be deemed to be mainly concentrated in the groove between the hills [17]. Then the local curvature at the groove of width  $b_g$  is a measure for the hydrostatic pressure  $p$ ,

$$p = \sigma_{xx} = \sigma_{yy} = \sigma_{zz} = -\frac{2\gamma}{b_g}, \quad (9)$$

per main radius of curvature, assuming idealized half spheres [18] (Fig. 4). Proposing concentric gaps around the individual surface clusters of radius  $R_C/2$  (area fraction:  $\frac{2b_g}{R_C}$ ) and an approximately hexagonal arrangement of the single clusters (Fig. 5), as shown by STM measurements, with equal area fractions of gaps joining two and three clusters (average sum of main radii of curvatures: factor 1.5), the tensile stresses in the late stages of film

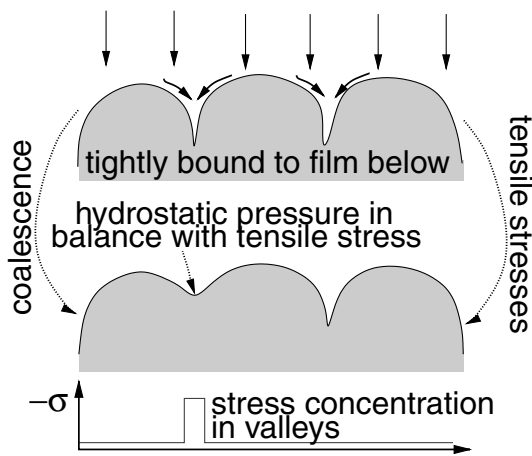


FIG. 4. Model for tensile stress generation due to continuous coalescence.

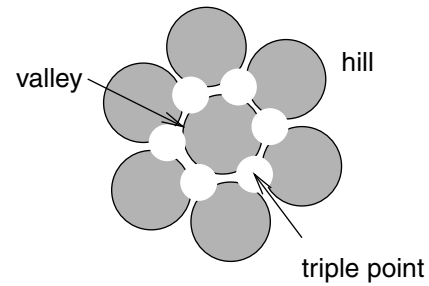


FIG. 5. Calculation of the mean radius of curvature in the grooves between the hills.

growth can be estimated to be

$$\langle \sigma \rangle = -1.5 \frac{2b_g}{R_C} \frac{2\gamma}{b_g} = -\frac{6\gamma}{R_C}. \quad (10)$$

Taking as a first approximation an area-weighted average value for  $\gamma$  in the case of alloys extrapolated with the temperature coefficient to the room temperature [19] and the lateral correlation length  $R_C$  determined from STM measurements (Fig. 1, [4,5]), experimental  $\sigma_E$  and model  $\sigma_M$  values for the late stages of film growth can be quantitatively compared, as shown in Table I. Even for very different correlation lengths and surface tensions, the agreement between experiments and model is extremely good for very different alloys, suggesting a universality of the proposed assumptions.

In literature [4,5], for describing the amorphous tensile stresses during late stages of growth, the Doljack-Hoffman grain boundary relaxation model [20] and the Murbach-Wilman freezing model [21] have been controversially discussed. The first assumes that tensile stresses originate from relaxation of the grain boundary structures in crystals, the latter by a freezing phase transition on top of surfaces. Suggesting continuous liquidlike hill coalescence, the presented model naturally combines the main ideas of both models. It should, however, be noted that for polycrystal systems additionally a grain-boundary energy should be taken into account.

Concerning the very early stages of single island film growth and subsequent coalescence, additional effects, based on the film-substrate interface and the capillarity, can be expected to contribute to the total observable stresses: Thermodynamically favored chemical reactions, such as Zr with the  $SiO_2$  substrate, can lead to stresses

TABLE I. Comparison of the absolute experimental values  $\sigma_E$  for the late-stage tensile stresses with the model predictions  $\sigma_M$ . The experimental lateral structure size  $R_C$  and the estimated surface energy  $\gamma$  are applied.

System	$R_C$ /nm	$\sigma_E$ /GPa	$\gamma$ /(N/m)	$\sigma_M$ /GPa
$Zr_{65}Al_{7.5}Cu_{27.5}$	19	0.58	1.739	0.55
CuTi	11	1.0	1.793	0.98
CoTb	10	0.7	1.276	0.76
$Zr_{35}Co_{65}$	9.2	$\approx 1.2$	2.117	1.38

by volume change during reaction, and—as shown by Spaepen [22]—including elastic forces for bending the substrate in the force equilibrium with capillary forces for single islands, a substrate curvature can be expected. Recently, Cammarata *et al.* [23] pointed out that, for a crystal system, a coupling by elasticity of stresses perpendicular to the substrate, such as grain boundary stresses, to the lateral strain during coalescence of a single island can lead to additional tensile or compressive stresses, depending on the Poisson ratio. The corresponding strains are propagated throughout the succeeding film due to the crystallinity. However, in the framework of a liquidlike coalescence model for amorphous films, the stress is solely determined by the shape of the surface after coalescence, erasing the history of the previous stress state completely. A comparable contribution to amorphous thin film stresses is therefore already implicitly included.

For a modeling of surface topography  $h(\vec{x}, t)$ , continuum-type rate equations of the shape

$$\frac{\partial h}{\partial t} = F[h] + \eta \quad (11)$$

(with the functional  $F[h]$  denoting a term of different spatial derivations of  $h$  to model surface processes and  $\eta$  being Gaussian white noise) have quantitatively successfully been applied [3,6]. Besides surface diffusion, and self-shadowing by atomic deflection, a  $(\nabla h)^2$  term has been shown to be necessary for quantitative modeling. The presence of viscous hill coalescence, leading to lateral structure broadening, suggests to identify the presence of the  $(\nabla h)^2$  term as the lowest order mathematical representation of hill coalescence, leading to lateral structure broadening. Furthermore,  $R_C$  is directly related to instability considerations in these continuum models [3], allowing predictions of late-stage tensile stresses from model parameters.

In summary, a model has been proposed based on local energy minimization on the surface. Surface reconstruction will be generally present, if surface stress and energy deviate, leading to morphology independent stress formation, primarily compressive stresses for most amorphous metals. Three dimensional, cusplike growth generates tensile stresses due to local energy minimization by viscous coalescence in a dynamic equilibrium of stress generation and surface energy reduction. Here, the cusplike structures may originate from island growth on top of a substrate, as observed in the early stages of growth, or due to clusterlike growth due to growth instabilities, such as self-shadowing. This is a direct link to continuum growth models, which

can quantitatively account for the growth characteristics of amorphous films, so that tailoring of structural and mechanical properties seems to be possible.

The authors acknowledge M. Moske, U. Herr, and the group of P. Hänggi for fruitful discussions, as well as the DFG-SFB 438 Augsburg-München, TP A1 for financial support.

---

\*Email address: smayr@gwdg.de

- [1] B. Reinker, M. Moske, and K. Samwer, *Phys. Rev. B* **56**, 9887 (1997).
- [2] S. G. Mayr, M. Moske, and K. Samwer, *Europhys. Lett.* **44**, 465 (1998).
- [3] S. G. Mayr, M. Moske, and K. Samwer, *Phys. Rev. B* **60**, 16 950 (1999).
- [4] M. Moske and K. Samwer, *Z. Phys. B* **77**, 3 (1989).
- [5] U. Geyer, U. von Huelsen, and H. Kopf, *J. Appl. Phys.* **83**, 3065 (1998).
- [6] M. Raible, S. G. Mayr, S. J. Linz, M. Moske, P. Hänggi, and K. Samwer, *Europhys. Lett.* **50**, 61 (2000).
- [7] R. J. Asaro and W. A. Tiller, *Metall. Trans. A* **3**, 1789 (1972).
- [8] J. W. Cahn, *Acta Metall.* **1333**, 1333 (1980).
- [9] R. Shuttleworth, *Proc. Phys. Soc. London Sect. A* **63**, 444 (1949).
- [10] R. C. Cammarata, *Prog. Surf. Sci.* **46**, 1 (1994).
- [11] H. Ibach, *Surf. Sci. Rep.* **29**, 193 (1997).
- [12] A. A. Griffith, *Philos. Trans. R. Soc. London A* **221**, 163 (1920).
- [13] W. D. Nix and B. M. Clemens, *J. Mater. Res.* **14**, 3467 (1999).
- [14] W. W. Mullins, *J. Appl. Phys.* **30**, 77 (1959).
- [15] W. M. Tong and R. S. Williams, *Annu. Rev. Phys. Chem.* **45**, 401 (1994).
- [16] H. Zhu, M. Ghaly, and R. S. Averback, in *Chemistry and Physics of Nanostructures and Related Non-Equilibrium Materials*, Proceedings of the Minerals, Metals and Materials Society (TMS) 1997 Annual Meeting, Orlando, FL, 1997, edited by E. Ma (TMS, Warrendale, 1997), p. 55.
- [17] C. Chiu and H. Gao, *Int. J. Solids Struct.* **30**, 2983 (1993).
- [18] L. D. Landau and E. M. Lifschitz, *Hydrodynamik* (Akademie-Verlag, Berlin, 1966).
- [19] N. Eustathopoulos, B. Drevet, and E. Ricci, *J. Cryst. Growth* **191**, 268 (1998).
- [20] F. A. Doljack and R. W. Hoffman, *Thin Solid Films* **12**, 71 (1972).
- [21] H. P. Murbach and H. Wilman, *Proc. Phys. Soc. London Sect. B* **66**, 905 (1953).
- [22] F. Spaepen, *J. Mech. Phys. Solids* **44**, 675 (1996).
- [23] R. C. Cammarata, T. M. Trimble, and D. J. Srolovitz, *J. Mater. Res.* **11**, 2468 (2000).